Electronic Supplementary Information

Tunable lattice dynamics and dielectric functions of two-dimensional Bi_2O_2Se: Striking layer and temperature dependent effects

Yafang Li,[a] Kai Dai,[a] Lichen Gao,[a] Jinzhong Zhang,*[a] Anyang Cui,[a] Kai Jiang,[a] Yawei Li,[a] Liyan Shang,[a] Liangqing Zhu[a] and Zhigao Hu*[a,b]

[a] Technical Center for Multifunctional Magneto-Optical Spectroscopy (Shanghai), Engineering Research Center of Nanophotonics & Advanced Instrument (Ministry of Education), Department of Physics, School of Physics and Electronic Science, East China Normal University, Shanghai 200241, China

[b] Collaborative Innovation Center of Extreme Optics, Shanxi University, Taiyuan, Shanxi 030006, China

* Correspondence: (J. Z. Zhang) jzzhang@ee.ecnu.edu.cn; (Z.G. Hu) zghu@ee.ecnu.edu.cn

List of Contents:

Supplementary Note 1

1. Optical microscope images:

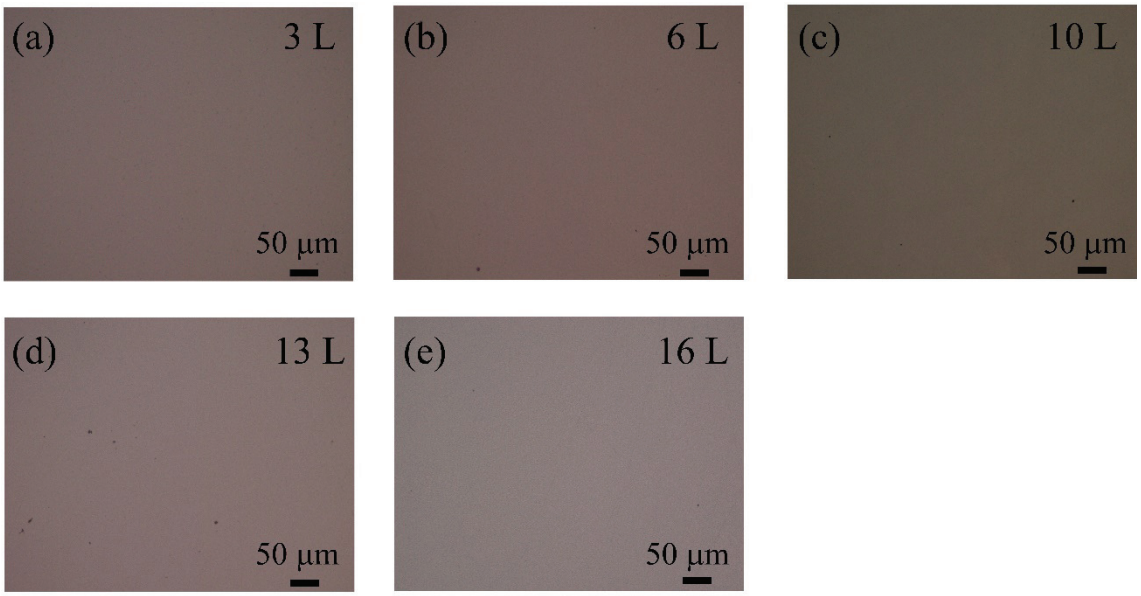

Fig. S1. (a)-(e) The basic optical microscope images of 3 L, 6 L, 10 L, 13 L, and 16 L Bi_2O_2Se films under 20× objective, respectively.

2. AFM images:

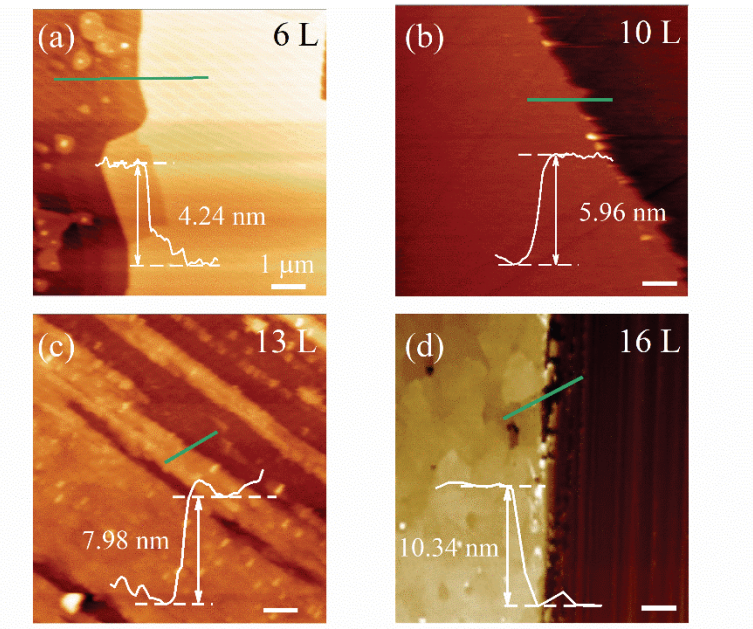

Fig. S2. (a)-(d) The AFM images of 6 L, 10 L, 13 L, and 16 L Bi_2O_2Se films, respectively.

Supplementary Note 2

XPS survey spectrum:

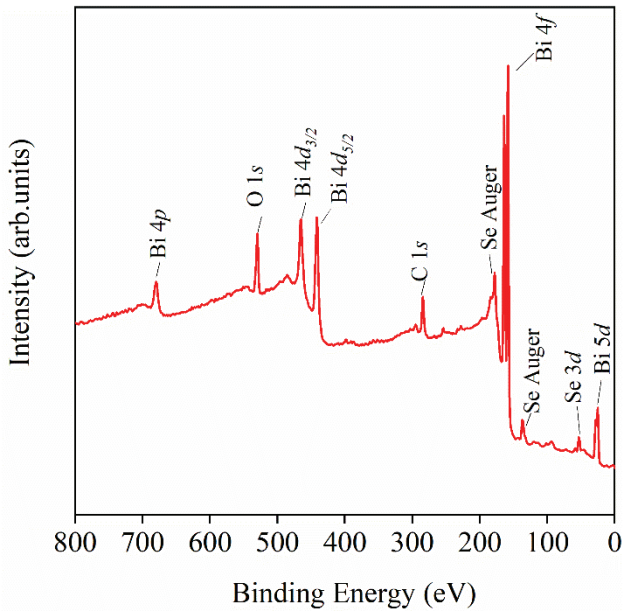

Fig. S3. The XPS survey spectrum of 10 L Bi_2O_2Se film.

Supplementary Note 3

Angle-resolved polarized Raman spectroscopy (ARPR):

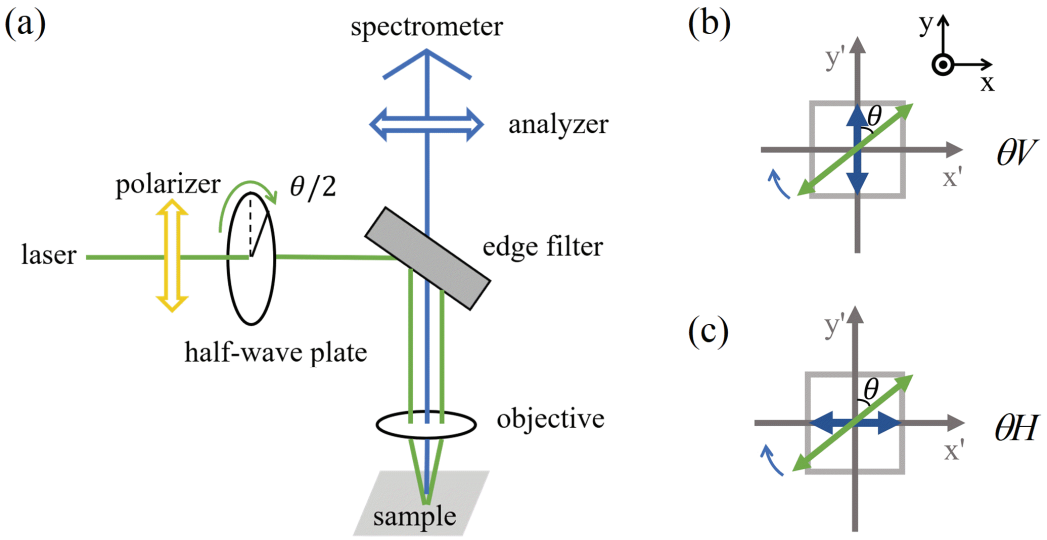

Fig. S4. (a) The schematic diagram of polarized Raman spectroscopy configuration. The schematic diagram of (b) θV and (c) θH configuration, respectively.

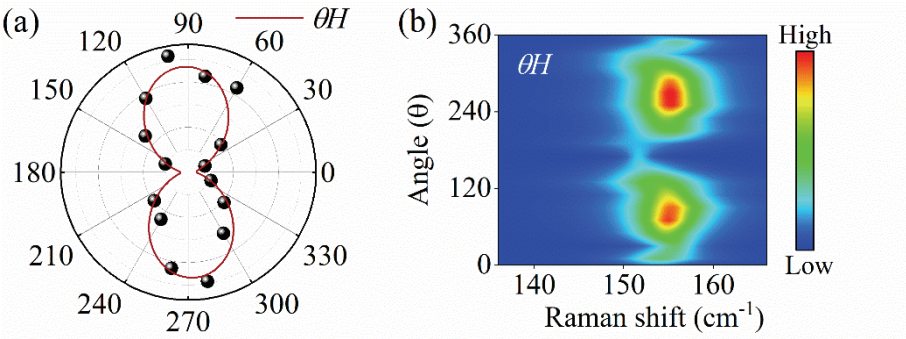

Fig. S5. (a) The polar plots and fitted intensities of A_{1g} Raman mode as the function of angles with θH configuration. (b) The polarized Raman mapping under θH configuration.

The ARPR measurement was carried out to further investigate the phonon anisotropy of 2D Bi_2O_2Se. As shown in Fig. S4, the half-wave plate was applied to change the polarization direction of incident light. The sample was kept stationary while rotating the half-wave plate in 20 steps. The analyzer can be selectively set to obtain the Raman scattering signals under the θV or θH configuration.

In these two polarized Raman configurations, the laboratory coordinates (x, y, z) which represented by black arrows coincides with crystal coordinates (x', y', z') referred as gray arrows in Fig. S4. In this case, by rotating the laser polarization direction, there is an angle (θ) between the laser polarization direction and one axis of the crystal coordinates. Furthermore, the incident laser polarization is rotated θ when the half-wave plate rotating $\theta/2$. As shown in Fig. S4b-c, the green arrows refer to the polarization direction of incident laser reaching the sample. The blue arrows represent vertical or horizonal direction of Raman signal selected by the analyzer before the spectrometer entrance. When $\theta = 0$, they correspond to the normal parallel (VV) and cross (VH) polarized Raman measurements, respectively. Therefore, the typical polarization configuration provides a convenient method to study crystal orientation and phonon anisotropy.

According to the Raman selection rules, the Raman intensity can be expressed as

$$I \propto |\hat{e}_S \cdot R \cdot \hat{e}_L|^2 \quad (1)$$

Where $\hat{e}_S$ and $\hat{e}_L$ represent the polarization vector of the Stokes scatter light and excitation light respectively, the R is the Raman tensor of one Raman mode.

The Raman tensors of A_{1g} mode is:

$$\begin{pmatrix} a & 0 & 0 \\ 0 & a & 0 \\ 0 & 0 & b \end{pmatrix}$$

In our ARPR measurement, $\hat{e}_L$ can be written as $(\sin\theta, \cos\theta, 0)$ for both two configurations, where θ denotes

the angle between the y axis and polarization direction. The $\hat{e}_S$ should be written as (0, 1, 0) for θV and (1, 0, 0) for θH configuration.

As a result, the Raman intensity of A_{1g} mode for θV follows the formula:

$$I_{\theta V} \propto \left| (0 \quad 1 \quad 0) \begin{pmatrix} a & 0 & 0 \\ 0 & a & 0 \\ 0 & 0 & b \end{pmatrix} \begin{pmatrix} \sin\theta \\ \cos\theta \\ 0 \end{pmatrix} \right|^2 = a^2 \cos^2\theta \tag{2}$$

And for θH follows:

$$I_{\theta H} \propto \left| (1 \quad 0 \quad 0) \begin{pmatrix} a & 0 & 0 \\ 0 & a & 0 \\ 0 & 0 & b \end{pmatrix} \begin{pmatrix} \sin\theta \\ \cos\theta \\ 0 \end{pmatrix} \right|^2 = a^2 \sin^2\theta \tag{3}$$

Supplementary Note 4

Layer-dependent bandgap:

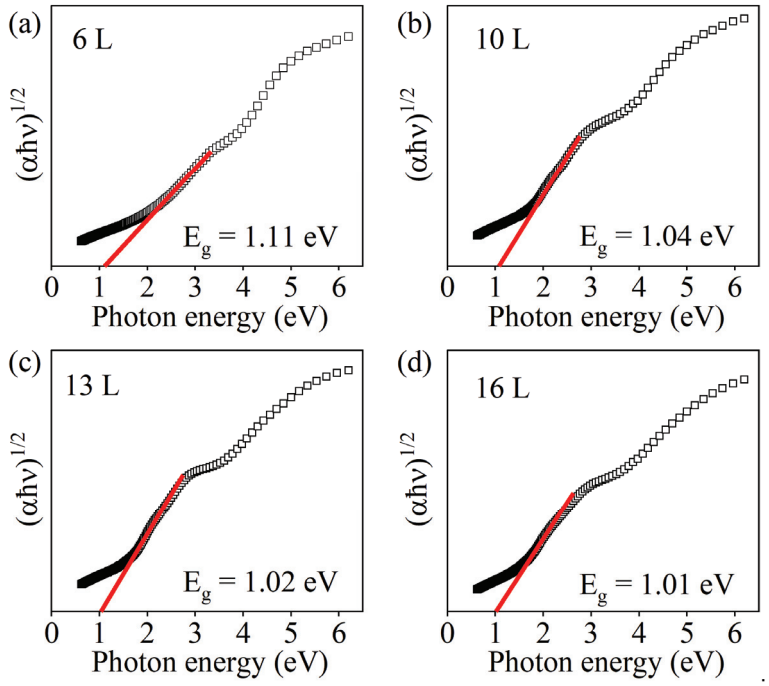

Fig. S6. (a)-(d) The Tauc plots of 6 L, 10 L, 13 L, and 16 L Bi_2O_2Se films.

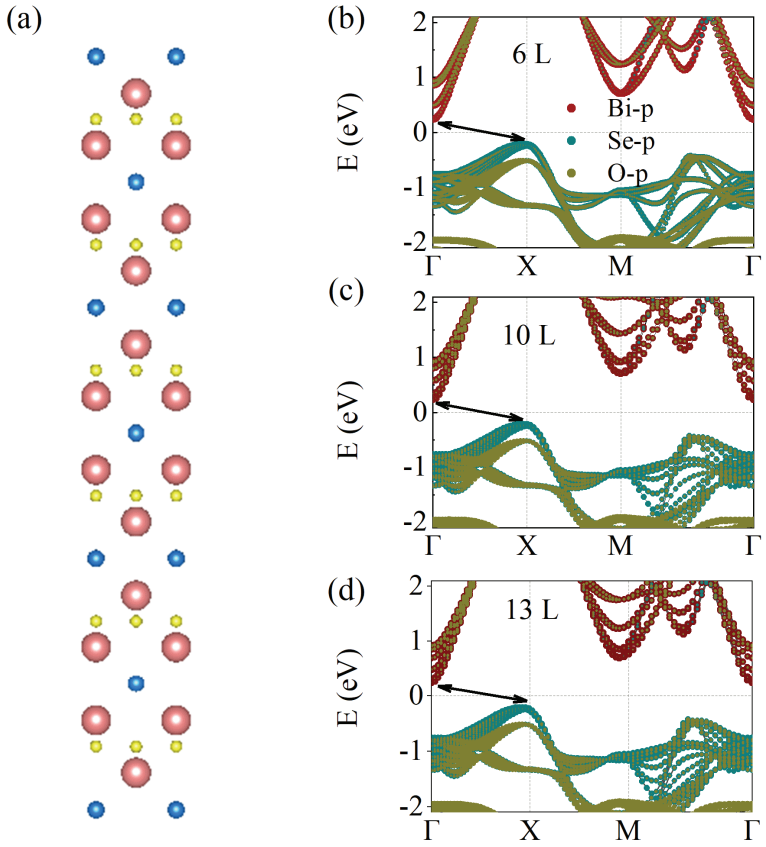

Fig. S7. (a) Atomic structure of 6 L Bi_2O_2Se calculated mode. (Pink, yellow, and bule balls correspond to Bi, O and Se atoms, respectively.) (b)-(d) The band structures of 6 L, 10 L, and 13 L Bi_2O_2Se films, respectively, while the dispersions of red, green, and yellow circles represent the contributions by Bi-*p*, Se-*p*, and O-*p* orbitals, respectively.

Supplementary Note 5

Temperature-dependent Raman spectroscopy

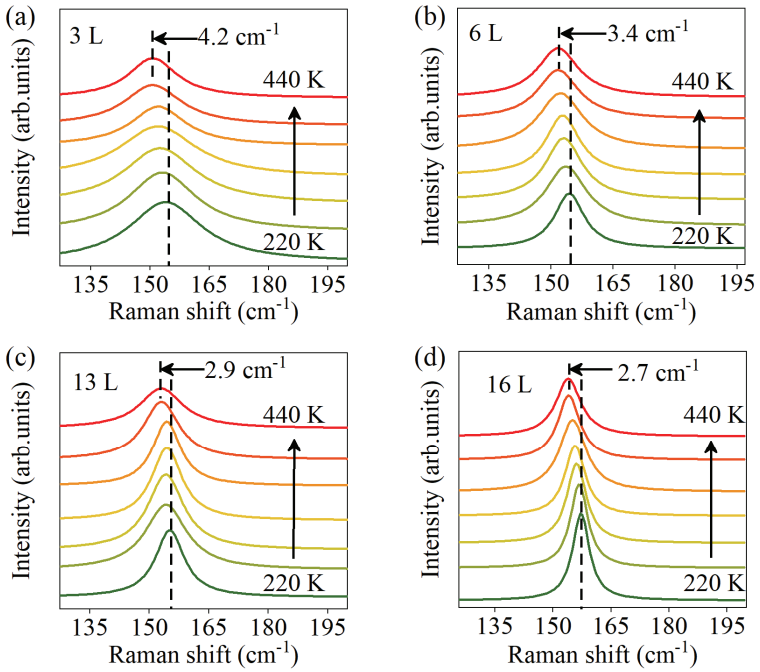

Fig. S8. The Raman spectra of (a) 3 L, (b) 6 L, (c) 13 L, and (d) 16 L Bi_2O_2Se from 220 K-440 K.

Supplementary Note 6

Spectroscopic ellipsometry analysis:

In this work, the spectra measured at different incident angles (60°, 65°, and 70°) have been fitted and shown in Fig. S8. The root means square error (RMSE) can evaluate the goodness of the SE fitted results, which is defined as:

$$\mathrm{RMSE}=\sqrt{\frac{1}{2M-P}\sum_{i=1}^{M}\left[\left(\Psi_{mea}^{i}-\Psi_{fit}^{i}\right)^{2}+\left(\Delta_{mea}^{i}-\Delta_{fit}^{i}\right)^{2}\right]} \quad (2)$$

M is the number of data points, and P is the number of unknown model parameters. Ψ_{mea}^{i} and Ψ_{fit}^{i} represent the ith measured and fitted amplitude, Δ_{mea}^{i} *and* Δ_{fit}^{i} represent the ith measured and fitted phase. Consequently, the RMSE values are 7.46, 1.58, 1.68, 7.31, and 4.71 of 3-16 L, respectively, which suggest reliable results.

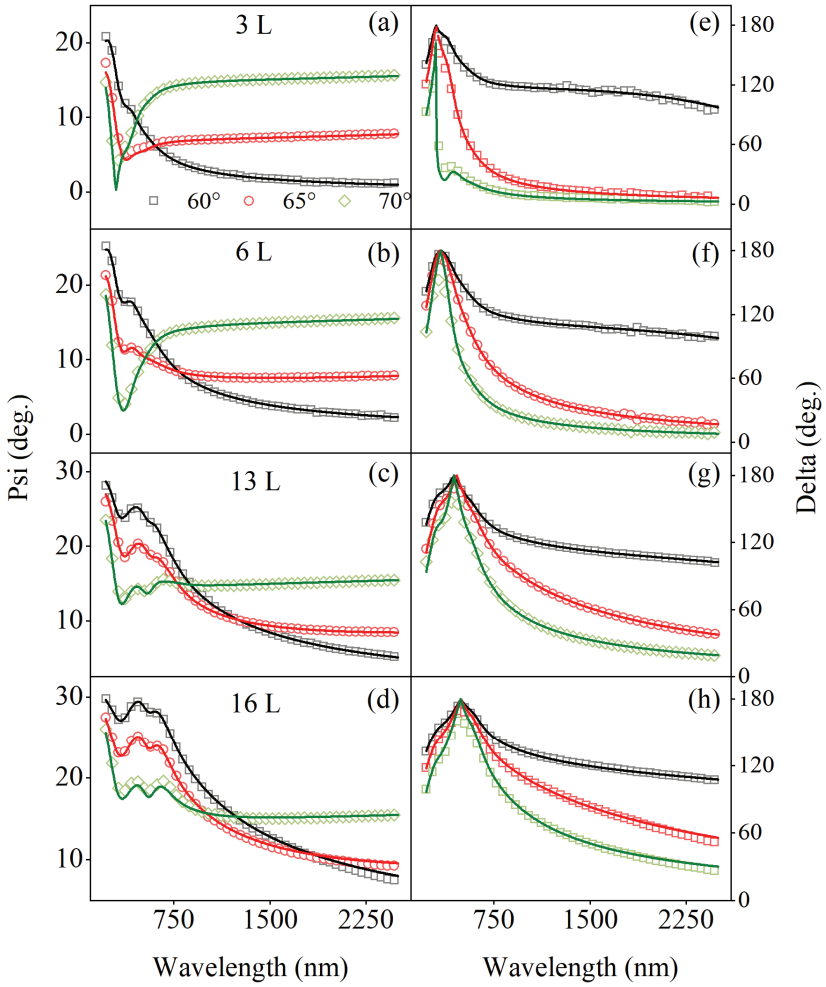

Fig. S9. The measured (symbols) and best-fitted (lines) Psi (a-d) and Delta (e-h) curves for 3 L, 6 L, 13 L, and 16 L Bi_2O_2Se films at 60°, 65°, 70° azimuthal orientation, respectively.

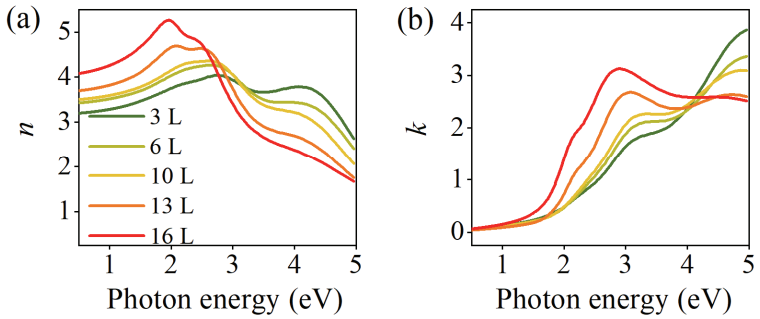

Fig. S10. The refractive index (a) and extinction coefficient (b) of Bi_2O_2Se films, respectively.

Table S1. The thickness of Bi_2O_2Se films measured by AFM and SE

Layer number		3 L	6 L	10 L	13 L	16 L
Thickness (nm)	AFM	1.94	4.24	5.96	7.98	10.34
	SE	2.12	3.81	5.83	7.95	9.88

Table S2. The parameters of SCP transitions well model for ultrathin Bi_2O_2Se films

Exciton	Parameters	3 L	6 L	10 L	13 L	16 L
E_a	A_0	0.95 (0.03)	0.97 (0.02)	0.83 (0.04)	1.48 (0.01)	2.53 (0.01)
	Φ_0 (deg)	140.21 (0.02)	140.22 (0.04)	140.59 (0.02)	141.20 (0.01)	141.01 (0.04)
	E_0 (eV)	2.21 (0.02)	2.19 (0.01)	2.12 (0.01)	2.09 (0.01)	2.04 (0.02)
	Γ_0 (eV)	0.57 (0.01)	0.47 (0.01)	0.38 (0.07)	0.27 (0.01)	0.27 (0.03)
E_b	A_1	3.41 (0.04)	4.55 (0.03)	6.73 (0.27)	10.23 (0.01)	9.89 (0.02)
	Φ_1 (deg)	134.64 (0.16)	134.66 (0.47)	134.52 (0.38)	134.46 (0.58)	134.35 (0.28)
	E_1 (eV)	2.96 (0.19)	2.93 (0.08)	2.84 (0.16)	2.71 (0.11)	2.48 (0.07)
	Γ_1 (eV)	0.56 (0.10)	0.59 (0.05)	0.58 (0.03)	0.52 (0.05)	0.52 (0.04)
E_c	A_2	18.35 (0.21)	14.63 (0.16)	11.78 (0.60)	9.31 (0.04)	8.55 (0.08)
	Φ_2 (deg)	128.67 (0.43)	128.75 (0.28)	128.73 (0.10)	127.71 (0.04)	129.55 (0.03)
	E_2 (eV)	4.58 (0.05)	4.54 (0.04)	4.47 (0.05)	4.08 (0.03)	4.02 (0.05)
	Γ_2 (eV)	0.93 (0.03)	0.97 (0.04)	1.01 (0.05)	0.98 (0.07)	1.62 (0.16)

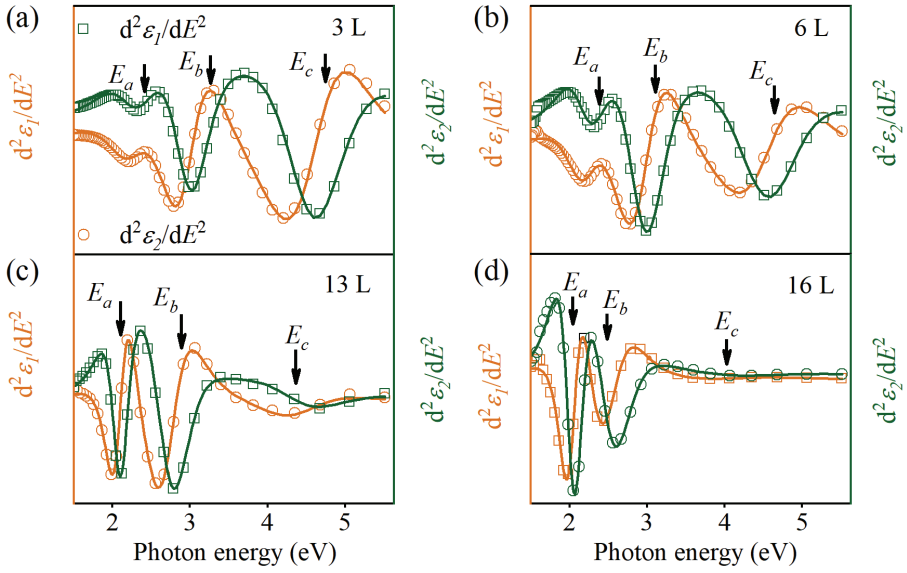

Fig. S11. (a)-(d) The second derivatives of the dielectric functions spectra (symbols) and the best-fitted spectra (lines) of 3 L, 6 L, 13 L, and 16 L Bi_2O_2Se film respectively. Three CPs including E_a, E_b, and E_c are marked by arrows.

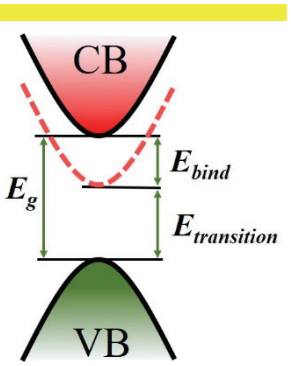

Fig. S12. The schematic diagram of the default local electronic band structure of 2D Bi_2O_2Se.

Table S3. The parameters of SCP model for ultrathin Bi_2O_2Se films at 230, 380, and 470 K, respectively

Samples		3 L			6 L			10 L			13 L			16 L		
T (K)		230	380	470	230	380	470	230	380	470	230	380	470	230	380	470
E_a	A_0	0.15 (0.04)	1.01 (0.01)	0.22 (0.06)	2.22 (0.03)	0.38 (0.04)	0.52 (0.02)	1.31 (0.02)	0.69 (0.01)	0.65 (0.02)	2.28 (0.01)	2.05 (0.02)	2.06 (0.01)	4.10 (0.01)	3.49 (0.01)	2.75 (0.01)
	Φ_0 (deg)	140.3 (0.1)	140.2 (0.1)	141.2 (0.1)	140.9 (0.1)	140.8 (0.1)	140.3 (0.1)	140.7 (0.1)	141.0 (0.1)	140.9 (0.1)	141.2 (0.1)	141.0 (0.1)	141.1 (0.1)	141.2 (0.1)	141.0 (0.1)	140.9 (0.1)
	E_0 (eV)	2.48 (0.01)	2.21 (0.01)	2.12 (0.04)	2.46 (0.02)	2.26 (0.07)	2.23 (0.01)	2.29 (0.03)	2.25 (0.01)	2.22 (0.01)	2.16 (0.02)	2.12 (0.03)	2.11 (0.02)	2.10 (0.02)	2.07 (0.02)	2.05 (0.02)
	Γ_0 (eV)	0.45 (0.02)	0.55 (0.01)	0.23 (0.01)	0.66 (0.02)	0.29 (0.05)	0.37 (0.01)	0.42 (0.01)	0.33 (0.01)	0.33 (0.01)	0.30 (0.03)	0.31 (0.04)	0.31 (0.03)	0.32 (0.04)	0.32 (0.04)	0.32 (0.03)
E_b	A_1	10.41 (0.16)	3.66 (0.02)	3.44 (0.01)	3.90 (0.06)	5.68 (0.06)	4.70 (0.05)	5.94 (0.05)	6.91 (0.04)	6.77 (0.04)	10.47 (0.03)	10.18 (0.04)	10.18 (0.03)	7.58 (0.01)	8.26 (0.02)	8.73 (0.02)
	Φ_1 (deg)	135.2 (0.2)	134.8 (0.1)	134.9 (0.1)	135.1 (0.1)	134.3 (0.1)	134.3 (0.1)	134.5 (0.1)	134.3 (0.1)	134.2 (0.1)	134.5 (0.1)	134.4 (0.1)	134.3 (0.1)	134.6 (0.1)	134.5 (0.1)	134.5 (0.1)
	E_1 (eV)	3.19 (0.25)	2.87 (0.10)	2.75 (0.06)	3.12 (0.29)	2.79 (0.40)	2.80 (0.34)	2.91 (0.33)	2.78 (0.30)	2.74 (0.30)	2.65 (0.03)	2.61 (0.05)	2.59 (0.03)	2.57 (0.10)	2.52 (0.13)	2.48 (0.17)
	Γ_1 (eV)	0.85 (0.04)	0.55 (0.01)	0.52 (0.04)	0.57 (0.01)	0.64 (0.03)	0.62 (0.06)	0.56 (0.05)	0.63 (0.04)	0.65 (0.06)	0.49 (0.09)	0.53 (0.06)	0.56 (0.02)	0.41 (0.06)	0.46 (0.08)	0.52 (0.08)
E_c	A_2	20.06 (0.01)	21.12 (0.08)	26.53 (0.02)	13.26 (0.02)	11.53 (0.04)	12.29 (0.07)	10.98 (0.02)	9.35 (0.02)	9.80 (0.20)	3.61 (0.10)	4.34 (0.02)	3.58 (0.02)	5.76 (0.01)	4.36 (0.14)	6.72 (0.12)
	Φ_2 (deg)	128.8 (0.1)	128.7 (0.6)	128.8 (0.1)	128.7 (0.5)	128.4 (0.1)	128.7 (0.1)	128.6 (0.3)	128.4 (0.7)	128.5 (0.3)	127.7 (0.1)	128.7 (0.5)	128.4 (0.1)	130.3 (0.1)	129.4 (0.2)	129.6 (0.2)
	E_2 (eV)	4.65 (0.03)	4.59 (0.18)	4.57 (0.16)	4.60 (0.04)	4.56 (0.02)	4.56 (0.08)	4.49 (0.03)	4.45 (0.05)	4.45 (0.07)	3.99 (0.05)	4.19 (0.06)	4.07 (0.04)	4.15 (0.01)	4.34 (0.06)	4.57 (0.08)
	Γ_2 (eV)	0.89 (0.02)	1.01 (0.04)	1.29 (0.02)	0.91 (0.01)	1.03 (0.02)	1.02 (0.01)	0.94 (0.01)	0.96 (0.01)	0.97 (0.02)	0.89 (0.05)	1.03 (0.02)	0.93 (0.08)	1.49 (0.03)	1.28 (0.05)	1.57 (0.03)

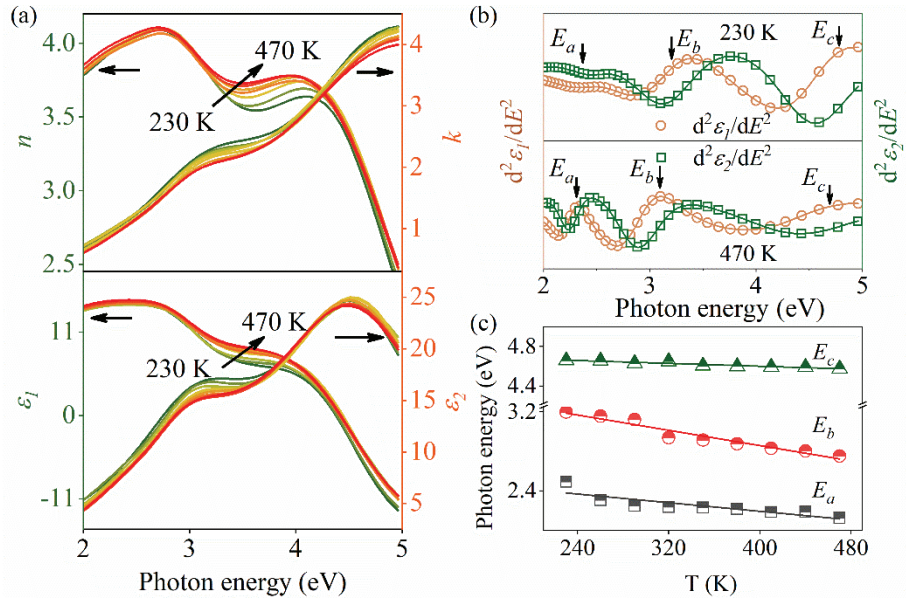

Fig. S13. (a) The refractive index, extinction coefficient, the real parts and the imaginary parts of dielectric function

of 3 L Bi_2O_2Se film from 230-470 K temperature. (b) The second derivatives of the dielectric functions spectra (symbols) and the best-fitted spectra (lines) of 3 L Bi_2O_2Se at 230 K and 470 K, respectively. Three CPs including E_a, E_b, and E_c are marked by arrows. (c) The center energies of three CPs versus temperature.

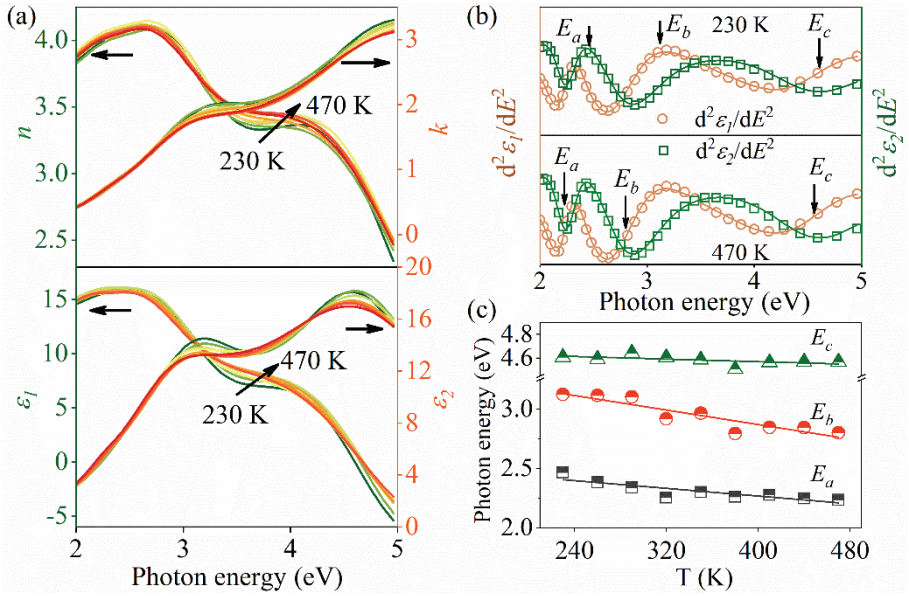

Fig. S14. (a) The refractive index, extinction coefficient, the real parts and the imaginary parts of dielectric function of 6 L Bi_2O_2Se film from 230-470 K temperature. (b) The second derivatives of the dielectric functions spectra (symbols) and the best-fitted spectra (lines) of 6 L Bi_2O_2Se at 230 K and 470 K, respectively. Three CPs including E_a, E_b, and E_c are marked by arrows. (c) The center energies of three CPs versus temperature.

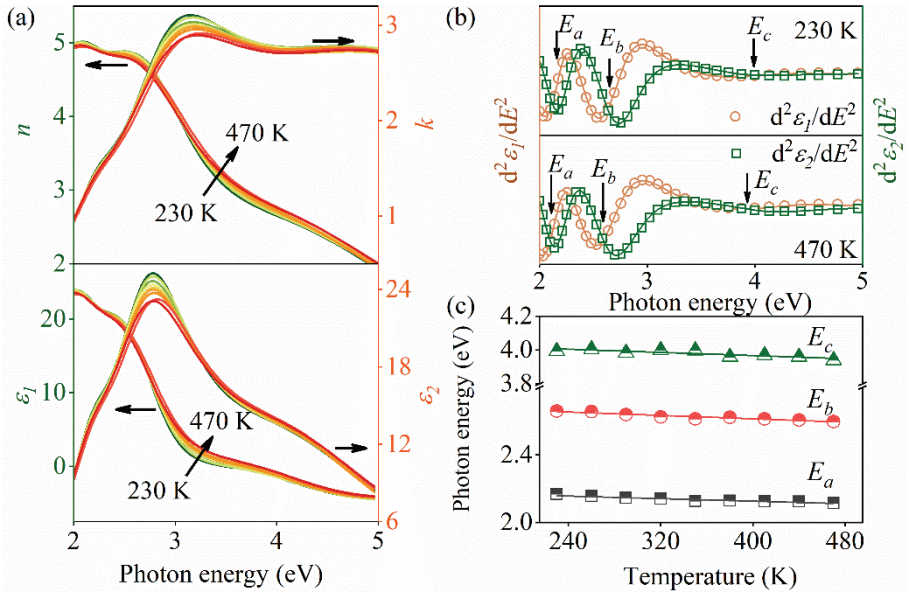

Fig. S15. (a) The refractive index, extinction coefficient, the real parts and the imaginary parts of dielectric function

of 13 L Bi_2O_2Se film from 230-470 K temperature. (b) The second derivatives of the dielectric functions spectra (symbols) and the best-fitted spectra (lines) of 13 L Bi_2O_2Se at 230 K and 470 K, respectively. Three CPs including E_a, E_b, and E_c are marked by arrows. (c) The center energies of three CPs versus temperature.

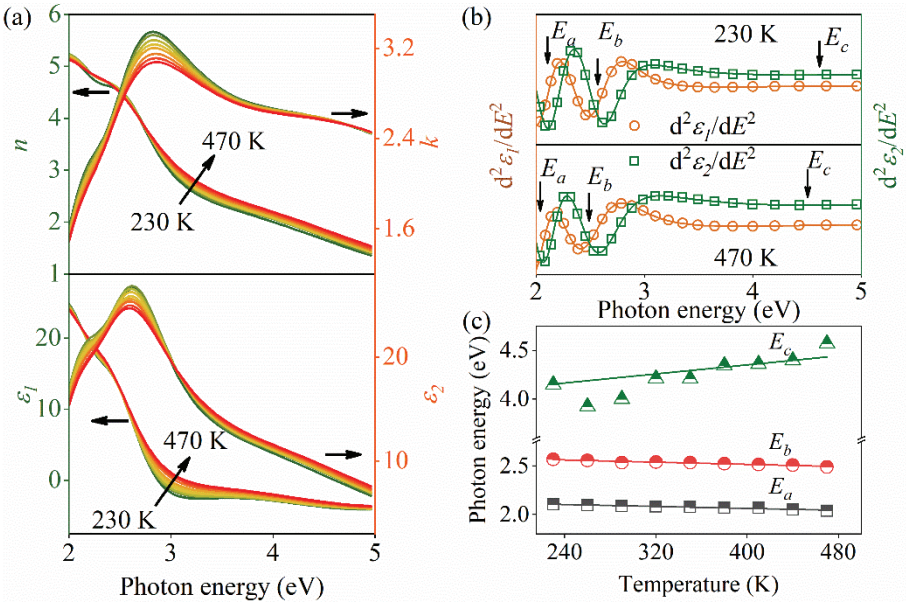

Fig. S16. (a) The refractive index, extinction coefficient, the real parts and the imaginary parts of dielectric function of 16 L Bi_2O_2Se films from 230-470 K temperature. (b) The second derivatives of the dielectric functions spectra (symbols) and the best-fitted spectra (lines) of 16 L Bi_2O_2Se at 230 K and 470 K, respectively. Three CPs including E_a, E_b, and E_c are marked by arrows. (c) The center energies of three CPs versus temperature.

Table S4. The temperature coefficient (-dE/dT) values of three CPs in Bi_2O_2Se films

Samples	E_a ($\times 10^{-4}$ eV/K)	E_b ($\times 10^{-4}$ eV/K)	E_c ($\times 10^{-4}$ eV/K)
3 L	-7.79	-19.30	-3.61
6 L	-7.29	-15.30	-3.28
10 L	-2.83	-8.47	-1.46
13 L	-2.72	-3.30	-2.43
16 L	-2.47	-2.83	——